Ocean Systems Engineering, *Vol. 3, No. 3 (2013) 237-255*
DOI: http://dx.doi.org/10.12989/ose.2013.3.3.237

A fuzzy controller based on incomplete differential ahead PID algorithm for a remotely operated vehicle

Junliang Cao[1], Hanjun Yin[2], Chunhu Liu[1] and Lian Lian[*1]

[1]*State Key Laboratory of Ocean Engineering, Shanghai Jiao Tong University (SJTU) Shanghai 200240, China*
[2]*Offshore Oil Engineering Co,LTD, Tianjin, China*

(Received August 21, 2013, Revised September 15, 2013, Accepted September 28, 2013)

Abstract. In many applications, Remotely Operated Vehicles (ROVs) are required to be capable of course keeping, depth keeping, and height keeping. The ROV must be able to resist time-variant external forces and moments or frequent manipulate changes in some specified circumstances, which require the control system meets high precision, fast response, and good robustness. This study introduces a Fuzzy-Incomplete Derivative Ahead-PID (FIDA-PID) control system for a 500-meter ROV with four degrees of freedom (DOFs) to achieve course, depth, and height keeping. In the FIDA-PID control system, a Fuzzy Gain Scheduling Controller (FGSC) is designed on the basis of the incomplete derivative ahead PID control system to make the controller suitable for various situations. The parameters in the fuzzy scheme are optimized via many cycles of trial-and-error in a 10-meter-deep water tank. Significant improvements have been observed through simulation and experimental results within 4-DOFs.

Keywords: ROV; fuzzy control; incomplete derivative ahead; FGSC

1. Introduction

Remotely Operated Vehicles (ROVs) are ideal and useful tools to accomplish various tasks which have increasing applications in exploring undersea environments, prospecting for mineral, and operating on the underwater structures. Operating in the deep sea, high precision trajectory and good maneuvering are required for most operating type ROVs. In considering of the highly non-linearized dynamic behaviors, accurate control of the ROV becomes very difficult, and is necessary for engineers and researchers involved. Therefore study the controlling of the ROV has become necessary for engineers and researchers in the last decades.

As tethered, teleoperated, power-supplied underwater vehicles (Nokin 1997, Nomoto and Hattori 1986), ROVs have been studied by researchers all over the world for decades. In order to guarantee ROVs are in good maneuvering condition and a high-precision trajectory along the pre-selected path under various uncertainties in practical applications such as internal and external frictions, damping and external disturbances (Fossen 1994), various advanced control techniques have been developed. Conventional PID controllers (Kuc 1998 and Li 2000) are used to control

*Corresponding author, Professor, E-mail: llian@sjtu.edu.cn

http://www.techno-press.org/?journal=ose&subpage=7 ISSN: 2093-6702 (Print), 2093-677X (Online)

functional manipulators and other dynamic systems; as well as fuzzy control (Antonelli and Chiaverini 2007), sliding-mode control (Bagheri and Moghaddam 2009a, Healey and Lienard 1993), nonlinear control (Nakamura and Savant 1992), adaptive control (Astrom and Wittenmark 1995, Nie *et al*. 2000), and neural network (Ishiii *et al*. 1998), have been proposed in literature. On the other hand, to ensure the static while operating, the dynamic positioning control system is also been introduced (Souza and Maruyama 2007).

Conventional PID-type controller is widely used in the past decades, which is designed for a limited situation for each group of parameters, in the meantime the vibration and quasi steady time are tough to reconcile. Conventional fuzzy control schemes require expert knowledge or many cycles of trial-and-error to achieve the desired performance (Moghaddam and Bagheri 2010). In the case of neural network control, training time is unpredictable and neural networks may not be suitable for real-time control (Shaw 1998). Both system-tracking stability and error convergence can be guaranteed in these neural-based-control systems. However, the high order term in the Taylor series, the functional reconstructed error, and the neural tuning weights are assumed to be known and bounded functions (Bagheri and Moghaddam 2009b).

The purpose of this study is to design a control system of ROVs to achieve the precise control of depth keeping, height keeping, and course keeping; meanwhile the robustness and practical reliability of the control system should be guaranteed as well. In this paper, a highly authentic mathematical ROV model is build, after that a control system applying to the ROV is designed so that simulation results are realism. This paper is organized as follows. The next section is ROV description, in which the 500-meter ROV is introduced including the hydraulic propulsion system and dynamic modeling in 4 degrees of freedoms (DOFs). In section 3, the authors introduce the specific design process of the Fuzzy Incomplete Derivative Ahead PID (FIDA-PID) controller. In section 4, the course keeping simulation results of the 500-meter ROV under possible occurrence of uncertainties are provided. In section 5, experimental and simulation results are shown including course keeping and depth keeping. Finally, the conclusions are given in section 6.

2. ROV description and modeling

This 500-meter ROV, as shown in Fig. 1, is designed to work within 500 m deep under the surface of sea, and aims at undersea searching, observing, and operating, as well as data collecting and recording. Automatic navigation function is required, which includes depth keeping, height keeping, and course keeping.

The main parameters of the 500-meter ROV are listed below

Table 1 Main parameters of the 500-meter ROV

Weight	Length	Width	height
1860 kg	2.473 m	1.3 m	1.5 m

To provide compellent simulation results, we have designed and preceded a series of hydrodynamic tests; some of the dimensionless hydrodynamic coefficients with the order of magnitude 10^{-3} are listed below (at constant test speed of V=1 m/s):

Fig. 1 500 meter-ROV

Table 2 Dimensionless coefficients

Coefficient	Value ($\times 10^{-3}$)	Coefficient	Value($\times 10^{-3}$)
$X_u^{'}$	-280.3	$Z_w^{'}$	-926.3
$X_{\dot{u}}^{'}$	-213.4	$Z_{\dot{w}}^{'}$	-488.9
$X_{u\|u\|}^{'}$	-400.5	$Z_{w\|w\|}^{'}$	107.6
$Y_v^{'}$	-499.6	$N_r^{'}$	-123.3
$Y_{\dot{v}}^{'}$	-305.2	$N_{\dot{r}}^{'}$	-25.25
$Y_{v\|v\|}^{'}$	-495.5	$N_{r\|r\|}^{'}$	-14.2
$I_z^{'}$	25.06		

2.1 Sensor system

The 500-meter ROV is equipped with a compass, a depthometer, an altimeter, and a gyroscope. The compass is able to measure the angle between heading and magnetic north, which is utilized as the control variable during course keeping. The depthometer is a pressure gauge in essence, which can provide the current depth of ROV transformed from the pressure. The altimeter is an acoustic susceptance which uses sonar to measure the current altitude. The gyroscope is able to measure angular acceleration and linear acceleration in x, y, and z direction, which may not be used in the control system directly but can supply assistant information to monitor the ROV's operating situation.

2.2 Propulsion system

The 500-meter ROV has six hydraulic propulsion thrusters marked with 1-6; four of which are equipped in the horizontal plane in the X-shape perpendicular to adjacent as shown in Fig. 2, and the remaining two thrusters are decorated in the top plane maintaining 10 degrees to the side plane.

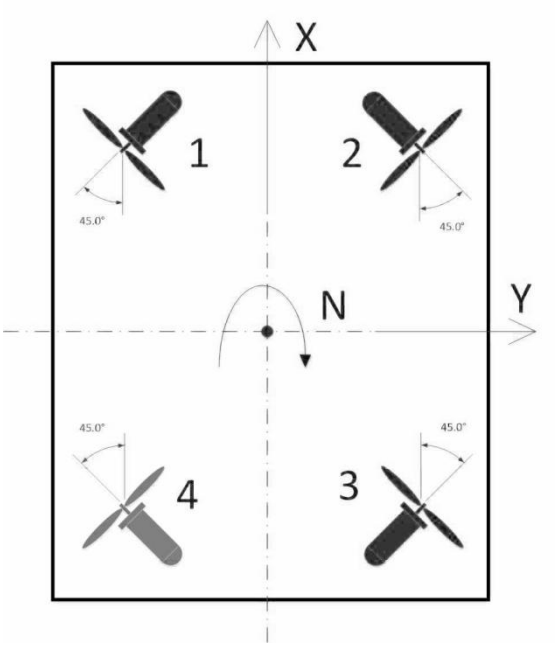

Fig. 2 The thruster configuration of the 500-meter ROV in the horizontal plane

The hydraulic propulsion thruster is able to generate a maximum thrust force of 1000 N while forward and 800 N while reversal. As a result of frictional resistance of the hydraulic valve, the thruster has a dead zone as shown in Fig. 3. Out of the dead zone the control voltage and the thruster control unit (TCU) pressure present a linear relationship as shown in Fig. 4.

The ROV is designed to move in any directions in the horizontal plane and turn head at the same time, in addition, it is symmetrical in all of three planes, so each thruster plays exactly the same role during movements. That means any of the thruster's stoppage would be able to represent all of the other three thrusters, which will be discussed in section 3 later. The thruster forces are marked with $\mathrm{u} = [u_1, u_2, u_3, u_4, u_5, u_6]^T$ which will compose into $\tau = [T_X, T_Y, T_Z, T_N]^T$, where T_X, T_Y, T_Z are forces in three directions and T_N is the moment in y-axis; and they have the flowing relationship in the body-fixed frame

$$\tau = \mathbf{Bu} \tag{2.1}$$

Where

$$\mathbf{B} = \begin{bmatrix} sin\phi & sin\phi & -sin\phi & -sin\phi & 0 & 0 \\ cos\phi & -cos\phi & -cos\phi & cos\phi & -cos\varphi & cos\varphi \\ 0 & 0 & 0 & 0 & sin\varphi & sin\varphi \\ l & -l & l & -l & 0 & 0 \end{bmatrix}$$

Where ϕ is the angle between the horizontal thrusters and x-axis; φ is the angle between

vertical thrusters and xy-plane; l is the operating distance between the thrusters and the center of gravity.

In order to allocate the thruster force to each propeller, the pseudo inverse matrix of B is needed, therefore

$$\mathbf{u} = \boldsymbol{B}^{\dagger}\boldsymbol{\tau} \tag{2.2}$$

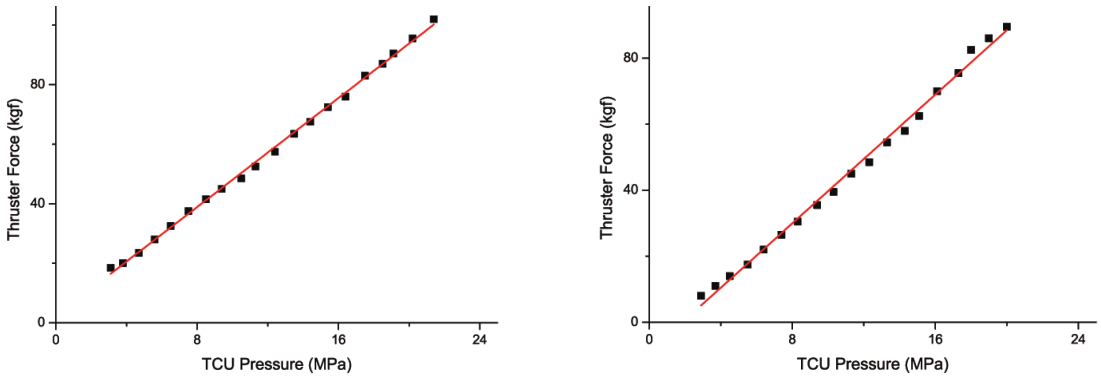

(a) (b)

Fig. 3 Linear fitting of TCU pressure versus thruster force while (a) forward and (b) reversal

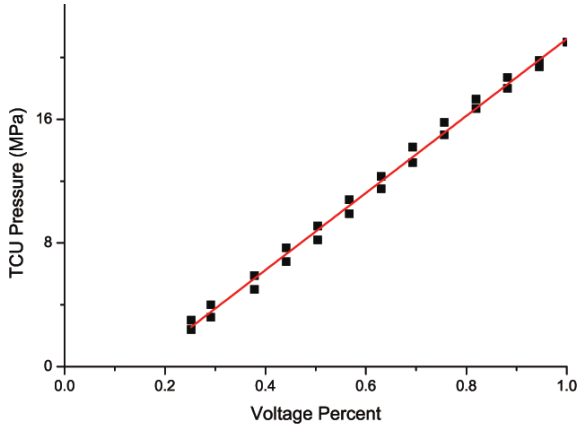

Fig. 4 Linear fitting of TCU pressure versus voltage percent of the thruster

2.3 Dynamic modeling

For simplicities, some rational assumptions are made for dynamic modelling (Bagheri and Moghaddam 2009b)

- ROV moves at low speed.

- The center of gravity and the center of buoyancy coincide with each other.
- The ROV is zero-buoyancy.
- The hydrodynamic coefficients are constant.
- The system is stable in pitch and roll therefore it is not necessary to control these DOFs.

In fact, the designed maximum velocity of 500-meter ROV is 2 knots which is relatively low; therefore the first assumption is reasonable. As long as the ROV has three symmetrical planes, the hydrodynamic coefficients higher than first order can be neglected. All of the dimensionless turns of hydrodynamic coefficients listed before are obtained through the experiment under the velocity of V=1 m/s, which is close to the maximum forward velocity, as constants.

The equation of motion of ROV has been given (Fossen 1994). In this paper, we use a 4-DOF nonlinear model based on Fossen outline, the mathematic ROV model in the body fixed frame can be represented as

$$\mathbf{M}\dot{\nu}+\mathbf{C}(\nu)\nu+\mathbf{D}(\nu)\nu+\mathbf{g}(\eta)=\boldsymbol{\tau}+\Delta\mathbf{f} \tag{2.3}$$

Where $\mathbf{M}$ is the inertia matrix including added mass $\boldsymbol{M_A}$, $\mathbf{C}(\mathbf{v})$ is the matrix of Coriolis and centrifugal terms; $\mathbf{D}(\mathbf{v})$ is the damping matrix; $\mathbf{g}(\boldsymbol{\eta})$ is the vector of gravitational forces and moments; $\boldsymbol{\tau}$ is used to describe the control input forces and moments acting on the vehicle in the body-fixed frame; $\Delta\mathbf{f}$ is the unknown 4-DOFs interference of force and torque mainly caused by ocean current, umbilical force, and reacting force of the passive arms. $\mathbf{v}$ denotes to velocities and angular velocity in the body fixed reference frame, $\mathbf{v}=[u,v,w,r]^T$. $\boldsymbol{\eta}$ is the position vector of ROV in 6-DOFs, which is

$$\eta=\left[\eta_1^T,\eta_2^T\right];\eta_1=\left[x,y,z\right]^T;\eta_2=\left[\phi,\theta,\psi\right]^T \tag{2.4}$$

The body fixed vector can be transformed into the earth fixed frame through the Euler angle transformation denoted by $\mathbf{J}(\boldsymbol{\eta})$ and can be expressed by

$$J(\eta)=\begin{bmatrix} J_1(\eta) & 0 \\ 0 & J_2(\eta) \end{bmatrix} \tag{2.5}$$

Therefore the kinematics equation of the ROV can be expressed by

$$\dot{\eta}=J(\eta)\nu \tag{2.6}$$

In many ROV applications, it is usually supposed that vehicle moves at low speed, since then, ROV is moving more stable and in this condition,, the hydrodynamic coefficients higher than first order and the coupled can be neglected. Combining the rigid body denoted by (RB) matrix and added mass matrix denoted by (A), the simplified expression of the parameter matrixes can be obtained

$$\mathbf{M}=\begin{bmatrix} m-X_{\dot{u}} & 0 & 0 & 0 \\ 0 & m-Y_{\dot{v}} & 0 & 0 \\ 0 & 0 & m-Z_{\dot{w}} & 0 \\ 0 & 0 & 0 & I_z-N_{\dot{r}} \end{bmatrix} \tag{2.7}$$

$$\mathbf{C}(\mathbf{v}) = \begin{bmatrix} 0 & 0 & 0 & -(m-Y_{\dot{v}})v \\ 0 & 0 & 0 & (m-X_{\dot{u}})u \\ 0 & 0 & 0 & 0 \\ (m-Y_{\dot{v}})v & -(m-X_{\dot{u}})u & 0 & 0 \end{bmatrix} \tag{2.8}$$

Damping forces at low speed motion could be assumed as a non-coupled, so the damping matrix can be expressed as

$$\mathbf{D}(\mathbf{v}) = -diag(X_u + X_{u|u|}\,|u|, Y_v + Y_{v|v|}\,|v|, Z_w + Z_{w|w|}\,|w|, N_r + N_{r|r|}\,|r|) \tag{2.9}$$

The quadratic damping force can be expressed into (Fossen 1994)

$$X_{u|u|}\,|u|\,u = \frac{1}{2}\rho C_{D_x} A_x\,|u|\,u \tag{2.10}$$

Therefore, the hydrodynamic damping force is expressed in a matrix based notation as

$$F_D = D(\dot{q})\dot{q} \tag{2.11}$$

where

$$\mathbf{D}(\dot{q}) = -\frac{1}{2}\rho\, diag(C_{D_x} A_x\,|u|, C_{D_y} A_y\,|v|, C_{D_z} A_z\,|w|, C_{D_r} A_r\,|r|)$$

The weight and buoyancy force can be expressed in the body-fixed coordinate frame

$$\mathbf{f}_G = J_1^{-1}(\eta_2)\{0, 0, mg\}^T \tag{2.12}$$

$$\mathbf{f}_B = -J_1^{-1}(\eta_2)\{0, 0, -\rho Vg\}^T \tag{2.13}$$

where m denotes the mass of the ROV, V denotes the volume of fluid displaced by the ROV, g is the acceleration gravity, and ρ is the fluid density. Since the 500-meter ROV is zero-buoyancy, finally the restoring force and moment vector in the body-fixed coordinate system is

$$\mathbf{g}(\eta) = \{0, 0, -(mg - \rho Vg), 0\} = 0 \tag{2.14}$$

2.4 Equation of motion

After modelling, we can express the equation of motion for the ROV in 4-DOFs

$$m(\dot{u} - vr) = X_{\dot{u}}\dot{u} - Y_{\dot{v}}vr + \frac{1}{2}C_{D_x} A_x\,|u| + T_x + F_x \tag{2.15}$$

$$m(\dot{v} + ur) = Y_{\dot{v}}\dot{v} - X_{\dot{u}}ur + \frac{1}{2}C_{D_y} A_y\,|v| + T_y + F_y \tag{2.16}$$

$$m(\dot{w}) = Z_{\dot{w}}\dot{w} + \frac{1}{2}C_{D_z}A_z \mid w \mid + T_z + F_z \tag{2.17}$$

$$I_z(\dot{r}) = N_{\dot{r}}\dot{r} + (X_{\dot{u}} - Y_{\dot{v}})uv + \frac{1}{2}C_{D_r}A_r \mid r \mid + T_n + M_n \tag{2.18}$$

where T_x, T_Y, T_z denote the resultant thrust forces in x, y and z direction; T_n denotes the resultant torque generated by thrusters in the xy-plane; F_x, F_Y, F_z, M_n denote the disturbance force and momentum that caused by cable tension and other environmental forces included by surface wave, wind, and ocean currents.

3. Controller design

Besides of the ROV body, the time delay of the thruster must be countered into consideration, which can be presented by

$$\mathrm{G_m(s)} = \frac{1}{T_m s + 1} \tag{3.1}$$

where T_m is the time delay of the thrusters.

3.1 State-space equation

In the case of stoppage happens to thruster 4, without loss of generality, the allocation matrix becomes to

$$\tilde{\mathbf{B}} = \begin{bmatrix} sin\phi & sin\phi & -sin\phi & 0 & 0 & 0 \\ cos\phi & -cos\phi & -cos\phi & 0 & -cos\varphi & cos\varphi \\ 0 & 0 & 0 & 0 & sin\varphi & sin\varphi \\ l & -l & l & 0 & 0 & 0 \end{bmatrix} \tag{3.2}$$

Consider the ROV model without interference force

$$\mathbf{M}\dot{\nu} + \mathbf{C}(\nu)\nu + \mathbf{D}(\nu)\nu = \boldsymbol{\tau} = \mathbf{Bu} \tag{3.3}$$

This can be easily transformed into the standard state-space equation

$$\dot{\nu} = -\mathbf{M}^{-1}[\mathbf{C}(\nu)\nu + \mathbf{D}(\nu)\nu] + \mathbf{M}^{-1}\mathbf{Bu} \tag{3.4}$$

Substituting the parametric matrixes we can obtain

$$\dot{\nu} = \mathbf{P}\nu + \mathbf{Q}\nu \mid \nu \mid + \mathbf{M}^{-1}\mathbf{Bu} \tag{3.5}$$

where **P** and **Q** are parameter matrixes derived from equation 2.15-2.18.

3.2 IDA-PID control

In this study, an Incompletion Differential (ID) combined with Differential Ahead (DA) PID controller is designed. Incompletion differential PID control is a modified PID control which adds a low pass filter $1/(1+T_f s)$ to the differential part in order to superstition the high frequency signal. In this case, this kind of controller can reduce the vibration causing by the instantaneous external interference.

The function of differential ahead PID control which does the derivative operation to the feedback signal but not the difference between input signal and feedback signal is to avoid vibration when the input changes frequently. Because the ROV driver may manipulated the hand shank frequently in some urgent situations.

3.3 Fuzzy gain seheduling controller

As a result of the boundedness of the conventional PID controller, for instance, the PID parameters of small angle-turn head movement and large one should be separated or oscillation even diverge of ROV might happen, a Fuzzy Gain Seheduling Controller (FGSC) (Talaq and Al-Basri 1999) should be adjunct to the IDA-PID controller to adapt its actions to the system behavior. Given the drawbacks of the previous solution, a Fuzzy-IDA-PID control system is proposed as shown in Fig. 5.

The idea is to find the fuzzy relationship between the 3 PID parameters and *E*\&*EC*, then modifying the parameters timely by detecting *E*&*EC* ceaselessly. The FGSC is able to satisfy various demands of the parameters in different *E*&*EC*, thereby the control system will be able to possess good dynamic/static performance.

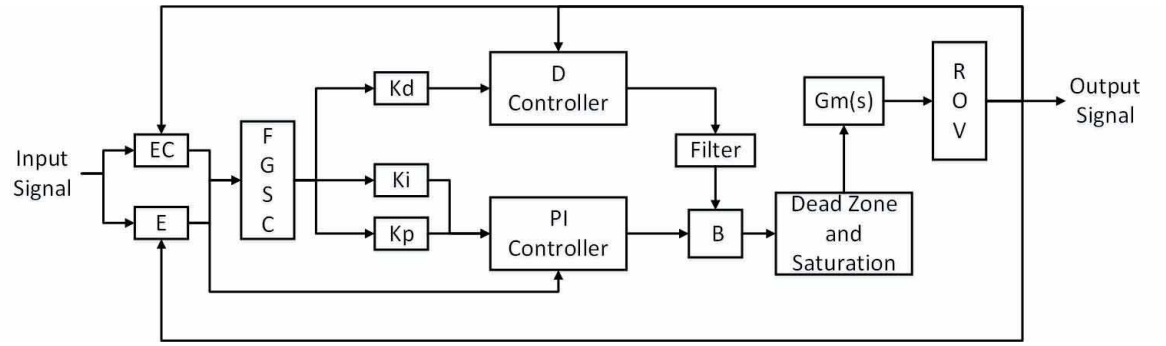

Fig. 5 Flow chart of FIDA-PID control system.

Inputs to the FGSC are *E* and *EC*; where *E* denotes the error between set value and actual value, and *EC* denotes the rate of change of error *E*.

- The set point error *E*=*R*-*C*, where *R* is the set value and *C* is the actual value
- The rate of change of error *EC*=$\frac{d}{dt}E$.

In this paper we use the absolutely value of *E*&*EC* to be the input linguistic variable, both of them have three elements.

Variable code

$$B \Rightarrow big, M \Rightarrow middle, S \Rightarrow small.$$

The membership function of navigation control is given in Figs. 6(a) and 6(b), where E is the error of heading angle and EC is the deviation ratio of heading angle.

The membership function of depth keeping and height keeping is given in Figs. 7(a) and 7(b), where *E* is the error of depth/height and *EC* is the deviation ratio of depth/height.

Assume there are five combinations of |*E*| and |*EC*|

1) |*E*| =*B*
2) |*E*| =*M* and |*EC*|=*B*
3) |*E*| =*M* and |*EC*|=*M*
4) |*E*| =*M* and |*EC*|=*S*
5) |*E*| =*S*

The degree of membership can be calculated by

1) $\mu_1(|E|,|EC|) = \mu_{BE}(|E|)$
2) $\mu_2(|E|,|EC|) = \mu_{ME}(|E|) \wedge \mu_{BC}(|EC|)$
3) $\mu_3(|E|,|EC|) = \mu_{ME}(|E|) \wedge \mu_{MC}(|EC|)$
4) $\mu_4(|E|,|EC|) = \mu_{ME}(|E|) \wedge \mu_{SC}(|EC|)$
5) $\mu_5(|E|,|EC|) = \mu_{SE}(|E|)$

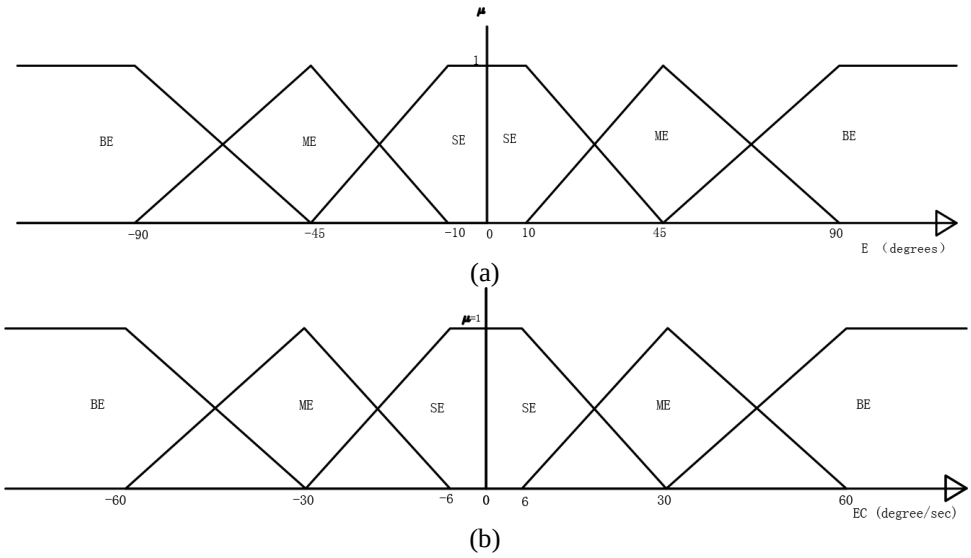

Fig. 6 Membership functions of (a) *E* and (b) *EC* in navigation control

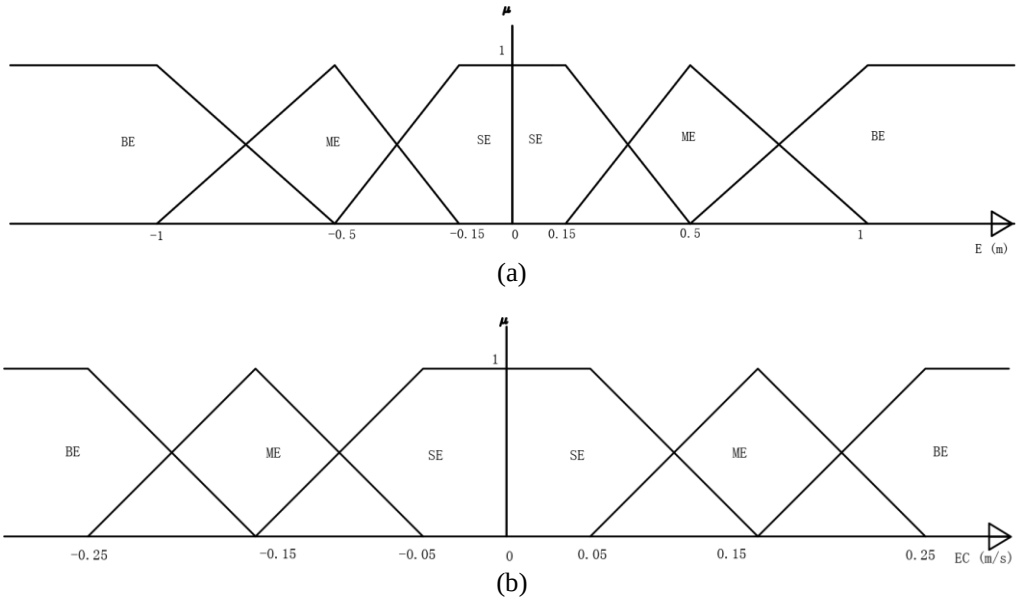

Fig. 7 Membership functions of (a) E and (b) EC in depth keeping/height keeping control

Thus K_P, K_I, K_D can be calculated according to the observed value of $|E|$ and $|EC|$ by the following equations

$$K_P = [\sum_{j=1}^{5} \mu_j(|E|,|EC|) \times K_{Pj}] / [\sum_{j=1}^{5} \mu_j(|E|,|EC|)] \tag{3.6}$$

$$K_I = [\sum_{j=1}^{5} \mu_j(|E|,|EC|) \times K_{Ij}] / [\sum_{j=1}^{5} \mu_j(|E|,|EC|)] \tag{3.7}$$

$$K_D = [\sum_{j=1}^{5} \mu_j(|E|,|EC|) \times K_{Dj}] / [\sum_{j=1}^{5} \mu_j(|E|,|EC|)] \tag{3.8}$$

where K_{Pj}, K_{Ij}, K_{Dj} are weighting factors of K_P, K_I, K_D in different states, whose value can be taken by

1) $K_{P1} = K'_{P1}$ $K_{I1} = 0$ $K_{D1} = 0$
2) $K_{P2} = K'_{P2}$ $K_{I2} = 0$ $K_{D2} = K'_{D2}$
3) $K_{P3} = K'_{P3}$ $K_{I3} = 0$ $K_{D3} = K'_{D3}$
4) $K_{P4} = K'_{P4}$ $K_{I4} = 0$ $K_{D4} = K'_{D4}$
5) $K_{P5} = K'_{P5}$ $K_{I5} = K'_{I5}$ $K_{D5} = K'_{D5}$

where $K_{P1}^{'} \sim K_{P5}^{'}$, $K_{I1}^{'} \sim K_{I5}^{'}$, and $K_{D1}^{'} \sim K_{D5}^{'}$ are the setting values of K_P, K_I, K_D in IDA-PID controller in different situations.

At the initial state, the value of the output signal will be regarded as zero. Then the degree of membership will be calculated according to the membership function, known as the FGSC module.

After that, K_P, K_I, K_D can be get through Eqs. (3.6) to (3.8), which will acting on the *D* controller and PI controller. The control results will act as the output signal; the difference between the input signal and it will generate the new generation of *E* and *EC* and have another control round. If the environment is stable, the difference between the input and output signal will be reduced smoothly, *E* and *EC* will become zero finally.

4. Simulation results

In the 500-meter ROV, $\phi = 45^{\circ}, \varphi = 80^{\circ}, l = 0.798m, T_m = 0.45s$, Thus we have

$$\mathbf{B}^{\dagger} = \begin{bmatrix} 0.354 & 0.343 & 0 & 0.313 \\ 0.354 & -0.343 & 0 & -0.313 \\ -0.354 & -0.343 & 0 & 0.313 \\ -0.354 & 0.343 & 0 & -0.313 \\ 0 & -0.084 & 0.508 & 0 \\ 0 & 0.084 & 0.508 & 0 \end{bmatrix}, \quad \tilde{\mathbf{B}}^{\dagger} = \begin{bmatrix} 0.707 & 0 & 0 & 0.627 \\ 0.687 & -0.667 & 0 & -0.018 \\ -0.020 & -0.667 & 0 & 0.609 \\ 0 & 0 & 0 & 0 \\ 0.082 & -0.164 & 0.508 & 0.073 \\ -0.082 & 0.164 & 0.508 & -0.073 \end{bmatrix}$$

The results of simulation using MATLAB software which is applied to control of an underwater vehicle model of the 500-meter ROV are presented in this section. The equation of motion for 4-DOFs of underwater vehicle was considered, and six hydraulic propulsion thrusters are used to control it in all four controllable DOFs.

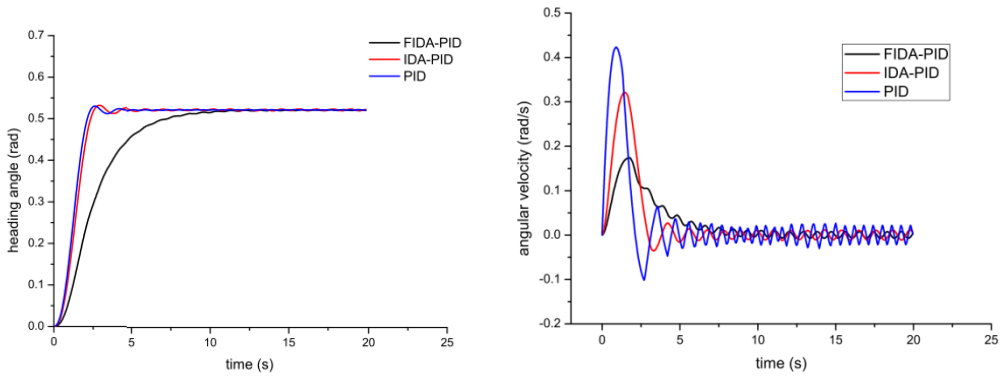

(a) (b)

Fig. 8 Heading angle (a) and angular velocity and (b) changes of three controllers by 30 degrees in situ

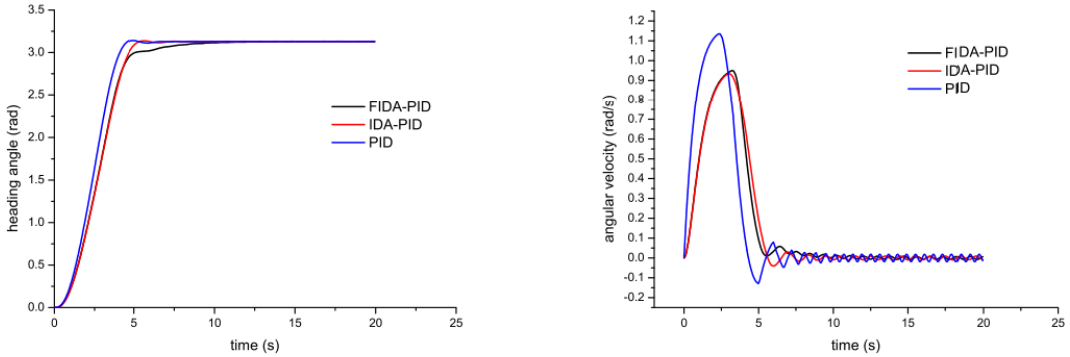

(a) (b)

Fig. 9 Heading angle (a) and angular velocity and (b) changes of three controllers by 180 degrees in situ

We can verify the parametric matrixes in the state function (Eq. (3.5))

$$\mathbf{P} = \text{diag}(0.246, 0.367, 0.51, 0.991)$$

$$\mathbf{Q} = diag(0.352, 0.364, -0.059, 0.282)$$

Conventional PID control, IDA-PID control, and Fuzzy-IDA-PID control are applied to the underwater vehicle model of the 500-meter ROV.

After many cycles of trial-and-error to achieve the desired performance, we finally find a group of parameters of the FIDA control system work well for the 500-meter ROV. The trial-and-error process is mainly based on the following rules:

- K_{P1} should be big in order to guarantee the control speed.
- K_D should be increased smoothly to guarantee the control sensitivity.
- K_{P5} should be neither too big to avoid vibration at the balance point, nor too small to avoid the loss of thrust force.
- The change of K_{P1} to K_{P5} should be smoothly, in order to avoid the vibration caused by the change of thrusters.

For course keeping control

$$\begin{aligned} K_{P1} &= 57 \quad K_{I1} = 0 \quad K_{D1} = 0 \\ K_{P2} &= 2 \quad K_{I2} = 0 \quad K_{D2} = 10 \\ K_{P3} &= 1 \quad K_{I3} = 0 \quad K_{D3} = 20 \\ K_{P4} &= 20 \quad K_{I4} = 0 \quad K_{D4} = 30 \\ K_{P5} &= 30 \quad K_{I5} = 0 \quad K_{D5} = 100 \end{aligned}$$

For height keeping control

$$K_{P1}=5000 \quad K_{I1}=0 \quad K_{D1}=0$$
$$K_{P2}=1000 \quad K_{I2}=0 \quad K_{D2}=500$$
$$K_{P3}=100 \quad K_{I3}=0 \quad K_{D3}=1000$$
$$K_{P4}=2000 \quad K_{I4}=0 \quad K_{D4}=2000$$
$$K_{P5}=3500 \quad K_{I5}=0 \quad K_{D5}=3500$$

Figs. 8 and 9 are the changes of heading angle and heading angular velocity with small/large turning angle in situ. Conclusion can be drawn that parameters of conventional PID control and IDA-PID control will not suitable for both cases; while the FIDA-PID control behaves well with no overshoot, no vibration, and has a proper response time.

Figs.10 and 11 are the changes of (a) heading angle, (b) heading angular velocity, (c) velocity in x-axis, and (d) velocity in y-axis with small/large turning angle while the ROV is moving forward. The FIDA-PID controller has significant improvements especially in small turning.

Fig.12 is the changes of (a) heading angle, (b) heading angular velocity, (c) velocity in x-axis, and (d) velocity in y-axis in the case of stoppage happens to thruster 4 at t=10s, and the control system adjust the allocation matrix at t=13s.

5. Experiment results

The results of experimental results of course keeping in situ and height keeping are presented in this section. The FIDA-PID control system of 500-meter ROV is verified in a 6-meter-deep (10-meters-deep maximum) water tank. Since the accuracy of CRS03-02 gyroscope is not as expected, the data of angular and linear velocities are not taken.

The parameters of FIDA control system are taken from the simulation process, which suit well in the experiments, barely difference can be observed.

Fig. 13 is the heading angle of course keeping in situ, changing from 51 degrees to 112 degrees, in which the experimental results of FIDA-PID control fit the desired value very well, while the two groups of conventional PID control systems generate either vibration or overshoot.

Fig.14 is the altitude of height keeping control, changing from 4.4 m (at surface) to 2.0 m; the bounce of height at the beginning of the control is because of the air bubble generated by the thrusters leading to the decrease of the water density.

6. Conclusions

In this paper, a FIDA-PID control system is designed in order to achieve a high-accuracy control for a remotely operated vehicle. A non-linear mathematic model highly close to the 500-meter ROV is build. Then, FGSC was combined with the IDA-PID control; the fuzzy control schemes are finally confirmed after many cycles of trial-and-error to achieve the desired performance. Course keeping is considered the most in instantaneous situations. From the simulation and experimental results, both course keeping and height keeping can achieve fast response, slight vibrations, and little overshoots.

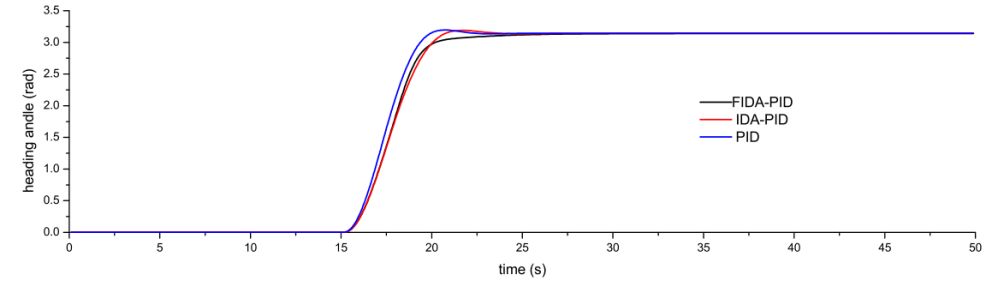

(a)

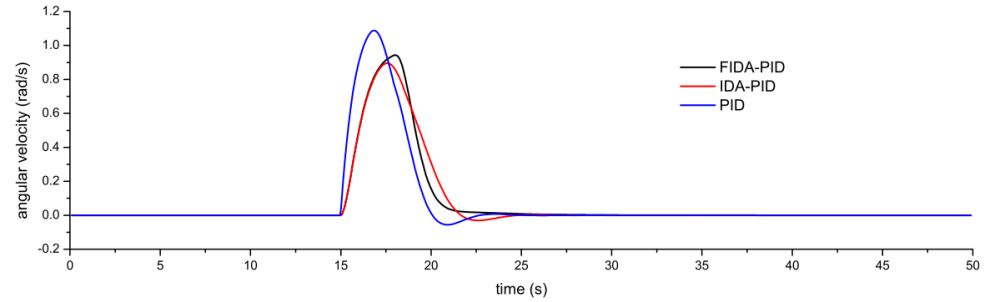

(b)

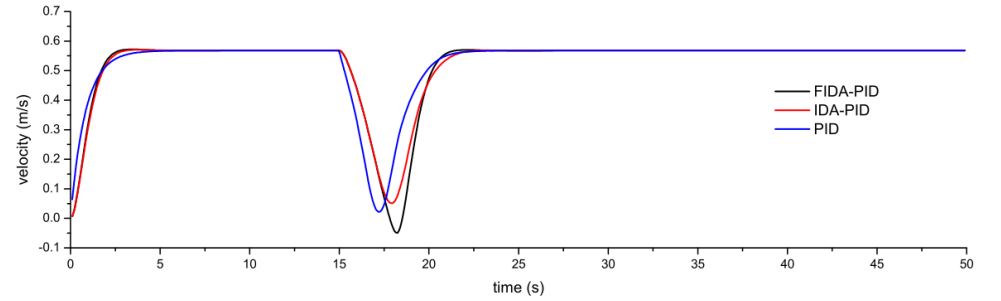

(c)

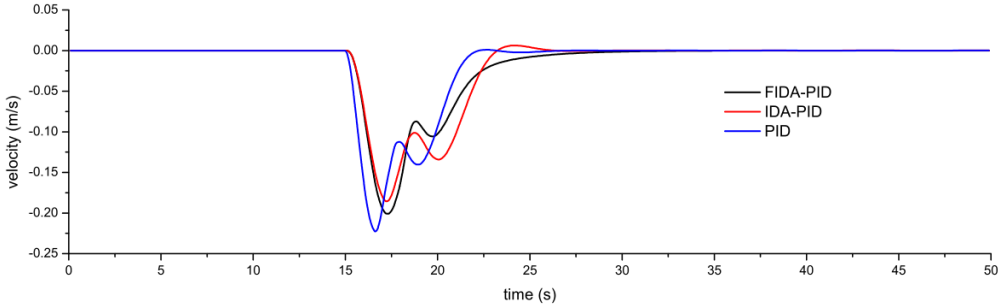

(d)

Fig. 10 Heading angle (a) angular velocity, (b) velocity in x-axis, (c) velocity in y-axis and (d) changes of three controllers by 180 degrees while the ROV is moving forward

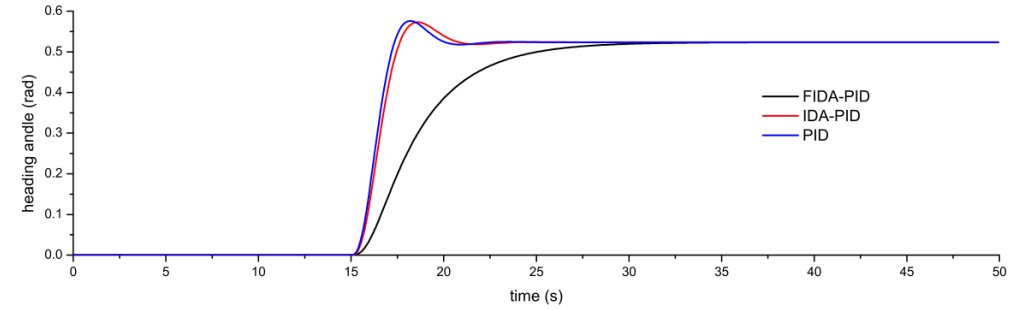

(a)

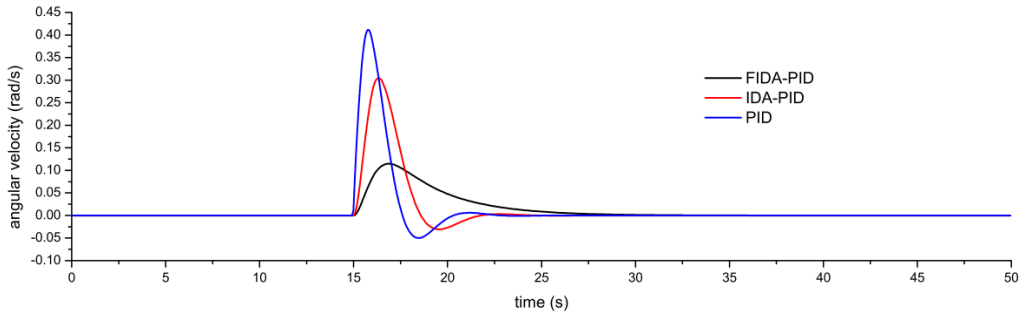

(b)

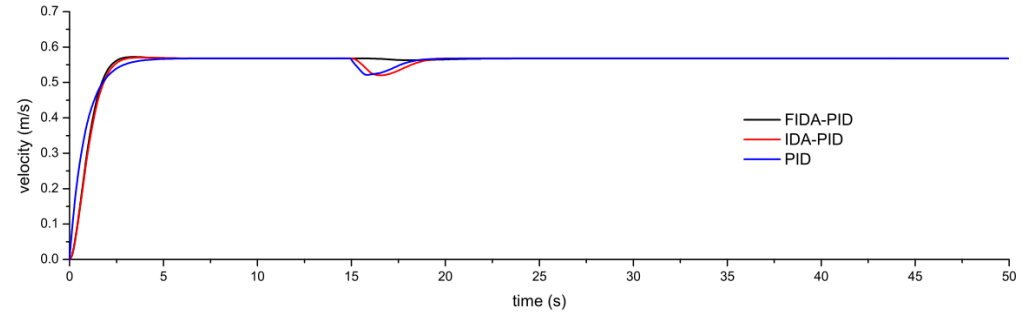

(c)

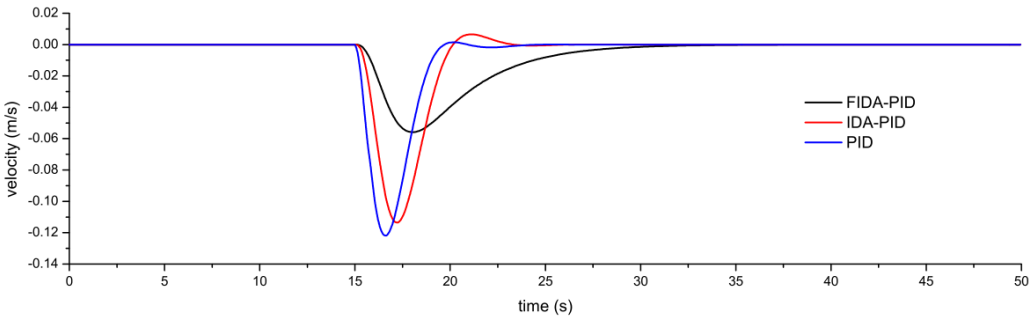

(d)

Fig. 11 Heading angle (a) angular velocity, (b) velocity in x-axis, (c) velocity in y-axis and (d) changes of three controllers by 30 degrees while the ROV is moving forward

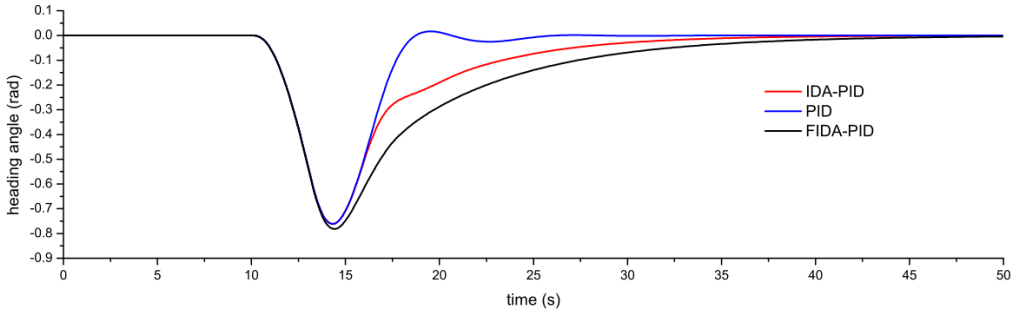

(a)

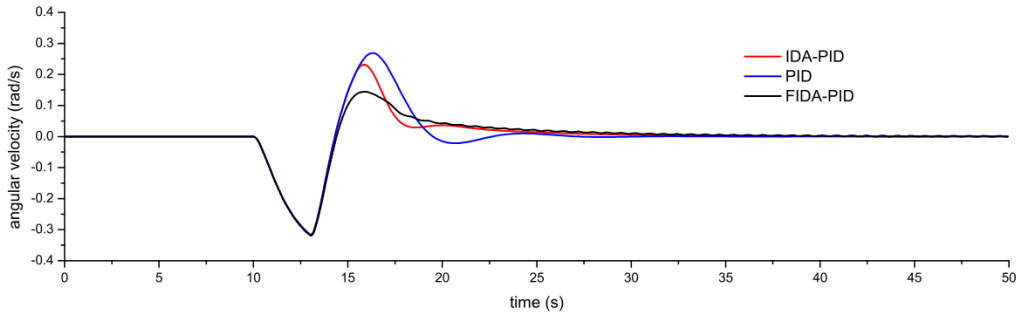

(b)

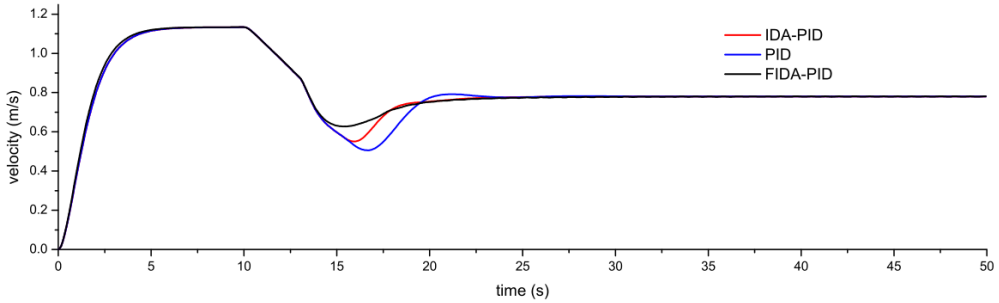

(c)

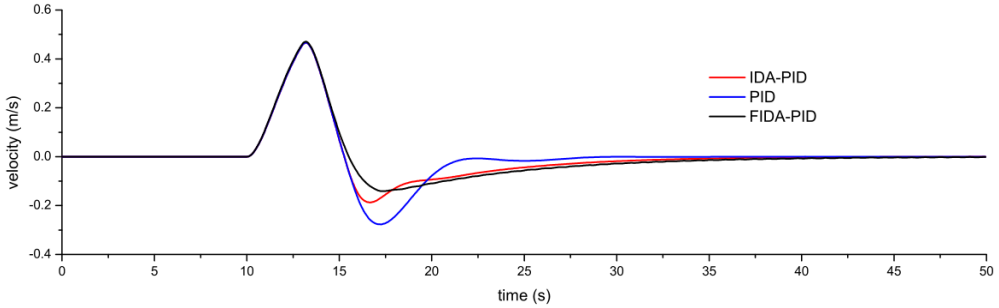

(d)

Fig. 12 Heading angle (a) angular velocity, (b) velocity in x-axis, (c) velocity in y-axis and (d) changes of three controllers in the case of stoppage happens to one thruster while the ROV is moving forward

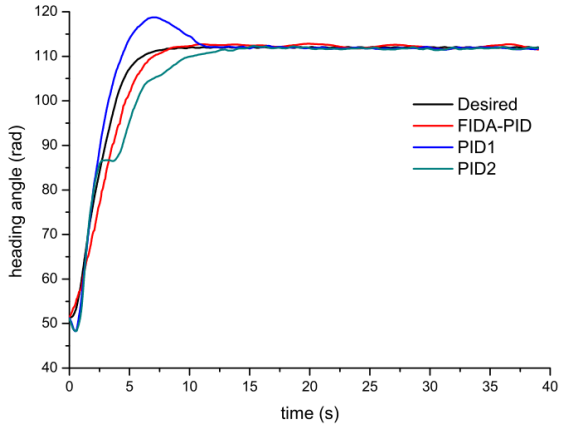

Fig. 13 Heading angle of experimental and simulation results

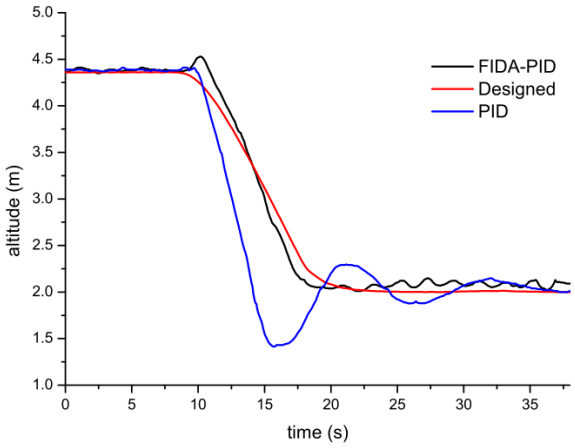

Fig. 14 Altitude of experimental and simulation results

Acknowledgments

This work is supported and sponsored jointly by the National Science and Technology Major Project of the Ministry of Science and Technology of China (Grant 2011ZX05027-005-003), the National High Technology Research and Development Program of China (863 Program)(Grant 2008AA092301-1), the National Natural Science Foundation of China (Grant 51279107), and the Science and Technology Commission of Shanghai Municipality (Grant 10DZ1210503).

References

Antonelli, G. and Chiaverini, S. (2007), "A fuzzy-logic-based approach for mobile robot path tracking, control engineering practice", *Fuzzy Syst*., **15**(2), 211-221.

Astrom, K.J. and Wittenmark, B. (1995), *Adaptive control*, New York, Addison-Wesley.

Bagheri, A. and Moghaddam, J.J. (2009a), "Simulation and tracking control based on neural-network strategy and sliding-mode control for underwater remotely operated vehicle", *Neurocomputing*, **72**, 1934-1950.

Bagheri, A. and Moghaddam, J.J. (2009b), "Decoupled adaptive neuro-fuzzy (DANF) sliding mode control system for a Lorenz chaotic problem", *Expert Syst. Appl*., **36**(3), 6062-6068.

De Souza, E.C. and Maruyama, N. (2007), "Intelligent UUVs: Some issues on ROV dynamic positioning", *Aerospace Elec. Syst*., **43**(1), 214-226.

Fossen, T.I. (1994), *Guidance and control of ocean vehicles*, Wiley, New York.

Healey, A.J. and Lienard, D. (1993), "Multivariable sliding mode control for autonomous diving and steering of unmanned underwater vehicles", *IEEE J. Oceanic Eng*., **18**(3), 327-339.

Ishiii, K., Fujii, T. and Ura, T. (1998), "Neural network system for online controller adaptation and its application to underwater robot", *Int. J. Robot. Autom*., **1**, 756-761.

Javadi-Moghaddam, J. and Bagheri, A. (2010), "An adaptive neuro-fuzzy sliding mode based genetic algorithm control system for under water remotely operated vehicle", *Expert Syst. Appl*., **37**, 647-660.

Kuc, T.Y. and Han, W.G. (1998), "Adaptive PID learning of periodic robot motion", *Proceedings of the IEEE Conference on Decision and Control*.

Li, Y., Ho, Y.K. and Chua, C.S. (2000), "Model-based PID control of constrained robot in a dynamic environment with uncertainty", *Proceedings of the IEEE International Conference on Control Applications*.

Nakamura, Y. and Savant, S. (1992), "Nonlinear tracking control of autonomous underwater vehicles", *Proceedings of the IEEE International Conference on Robotics and Automation*.

Nie, J., Yuh, J. and Fossen, T.I. (2000), "On-board sensor-based adaptive control of small UUVs in very shallow water", *Int. J. Adapt. Control*, **14**, 441-452.

Nokin, M. (1997), "Victor 6000 a deep teleoperated system for scientific research", *Proceedings of the OCEANS'97, MTS/IEEE Conference*.

Nomoto, M. and Hattori, M. (1986), "A deep ROV DOLPHIN 3K: design and performance analysis", *IEEE J. Oceanic Eng*., **11**(3), 373-391.

Shaw, I.S. (1998), *Fuzzy control of industrial systems-Theory and applications*, Dordrecht, Kluwer Academic Publishers.

Talaq, J. and Al-Basri, F. (1999), "Adaptive fuzzy gain scheduling for load frequency control", *IEEE T. Power Syst*., **14**, 145-150.